Journal of the Serbian Chemical Society
JSCS-info@shd.org.rs • www.shd.org.rs/JSCS
J. Serb. Chem. Soc. *89* (1) 63–77 (2024)
JSCS–5706
Original scientific paper
Published 12 February 2024

[BMIm][PF6]/silicon oil/multi-walled carbon nanotubes paste electrode: Electrochemical properties and application for lead and cadmium ion determinations

HAI D. TRAN[1], UYEN P. N. TRAN[2] and DINH QUAN NGUYEN[3,4]*

[1]Faculty of Environment, Ho Chi Minh University of Natural Resources and Environment, Ho Chi Minh City, Vietnam, [2]Faculty of Engineering and Technology, Van Hien University, Ho Chi Minh City, Vietnam, [3]Laboratory of Biofuel and Biomass Research, Faculty of Chemical Engineering, Ho Chi Minh City University of Technology (HCMUT), 268 Ly Thuong Kiet, District 10, Ho Chi Minh City, Vietnam and [4]Vietnam National University Ho Chi Minh City, Linh Trung Ward, Thu Duc District, Ho Chi Minh City, Vietnam

(Received 22 June, revised 21 July, accepted 11 December 2023)

Abstract: The electroanalytical methods have been developed for wide application, especially for trace metal ions. In this study, the applicability of 1-butyl--3-methylimidazolium hexafluorophosphate ([BMIm][PF6]) ionic liquid as a pasting binder to fabricate a multi-walled carbon nanotube paste electrode (MWCNT PE) for detecting Pb^{2+} and Cd^{2+} was evaluated. The electrochemical properties of electrodes were explored by cyclic voltammetry, electrochemical impedance spectroscopy and linear sweep anodic stripping voltammetry. The use of [BMIm][PF6] alone as a conductive binder resulted in an electrode that was unsatisfactory for electrochemical analysis. However, the MWCNT PE with the pasting mixture of silicon oil and [BMIm][PF6] displayed excellent sensitivity for the Pb^{2+} and Cd^{2+} determinations, with limits of detection of 2.25 and 1.59 μg L^{-1}, respectively. The proposed electrode was demonstrated to be a reliable sensor for accurately quantifying trace amounts of Pb^{2+} and Cd^{2+}, exhibiting good repeatability, reproducibility and stability.

Keywords: capacitive current; heavy metal; electrochemical analysis; cyclic voltammetry; anodic stripping voltammetry.

INTRODUCTION

Heavy metals are essential micronutrients for living organisms in small amounts. However, they become toxic when their concentrations exceed certain thresholds.[1–3] The common heavy metals in water are arsenic, cadmium, chromium, lead, copper, nickel and zinc. These metals can damage the brain, lungs, kidneys, liver, blood composition and other organs.[1] In the long term, heavy

* Corresponding author. E-mail: ndquan@hcmut.edu.vn
https://doi.org/10.2298/JSC230622095G

metals can also damage DNA repair pathways and protein function, which can have a negative impact on the genetic basis of organisms.[4] Therefore, analytical techniques have been developed for monitoring trace heavy metal ions in water.

Electrochemical analysis is a powerful technique for the trace determination of analytes, especially heavy metals.[5–7] Electrical signals generated from redox reactions on the working electrode surface are transferred to an electronic device that records the variability of electrical parameters.[8,9] Therefore, the electrochemical properties of the working electrode play an important role in the sensitivity and selectivity of electroanalysis.

Among popular electrode types, carbon paste electrodes (CPEs) are widely applicable because of their low background current, ease of preparation, simple renewal, cost-effectiveness and high feasibility.[10,11] Graphite,[12] glassy carbon,[13] diamond,[14] carbon nanofiber[15] and multi-walled carbon nanotubes (MWCNTs)[16] have been applied for constructing a CPE. MWCNTs have been shown to have interesting electrochemical properties, such as large electroactive sites, chemical inertness, a fast electron transfer rate and functional flexibility.[17,18] These properties demonstrate that MWCNTs are a promising material for CPEs. However, the sensitivity of CPEs is often limited by the presence of a non-electrical conductive binder in the paste composite.[19] Gou *et al.* fabricated a MWCNT tower electrode using a polystyrene binder and found a limit of detection (*LOD*) of 2.48 and 2.8 μg L^{-1} for Pb^{2+} and Cd^{2+}, respectively.[20] In a study by Tarley *et al.*,[21] a MWCNT PE with mineral oil binder was constructed, achieving an *LOD* of 6.6 μg L^{-1} for Pb^{2+} and 8.4 μg L^{-1} for Cd^{2+}. The higher *LOD*s of 1.31 mg L^{-1} for Pb^{2+} and 47 μg L^{-1} for Cd^{2+} at the MWCNT PE using paraffin oil binder were reported.[22]

Ionic liquids (ILs) have recently been proposed as an effective pasting binder for CPEs due to their high chemical and thermal stability, negligible vapour pressure and high conductivity.[19,23] IL-CPEs exhibit enhanced electrochemical responses for analytical applications.[23] Ping *et al.* reported that the bismuth film-modified graphite PE using *n*-octylpyridinium hexafluorophosphate binder achieved an *LOD* of 0.12 μg L^{-1} for Pb^{2+} and 0.1 μg L^{-} for Cd^{2+}.[24] In a careful procedure, a pasting mixture of acid-treated MWCNTs, graphite and triphenylphosphine was used to fabricate PE, which can detect Pb^{2+} and Cd^{2+} at low *LOD*s of 0.012 μg L^{-1} for Pb^{2+} and 0.008 μg L^{-1} for Cd^{2+}.[25] Yang *et al.* used a suspension of NH_2-functionalized SnO_2 nanowire and $[C_4dmim][NTf_2]$ to modify the surface of a glassy carbon electrode for Cd^{2+} determinations with an *LOD* of 0.6 μg L^{-1}.[26] More recently, bismuth nanoparticle-modified PE based on carbon nanofibers/$[EMIm][NTf_2]$/paraffin oil/graphite composite was shown to be effective for Pb^{2+} and Cd^{2+} detections, achieving *LOD*s of 0.12 and 0.25 μg L^{-1}, respectively.[27]

This study presented a simple protocol to prepare a PE using pristine MWCNTs and a mixture of [BMIm][PF6] and silicon oil as a pasting binder for individual determinations of Pb^{2+} and Cd^{2+}. The effects of [BMIm][PF6] on the electrochemical behaviour of the fabricated PE were explored. The proposed electrode was applied for detecting Pb^{2+} and Cd^{2+} in simulated solutions and tap water using linear sweep anodic stripping voltammetry (LSASV). The reliability, repeatability and reproducibility of the proposed electrode were also evaluated.

EXPERIMENTAL

Reagents and materials

MWCNTs were synthesized by the chemical vapor deposition technique and supplied by Vinanotech (Vietnam). Silicon oil, *n*-hexane, and potassium chloride (KCl) were obtained from Merck. Potassium hexacyanoferrate ($K_3Fe(CN)_6$), lead, and cadmium nitrate salts were purchased from Sigma. All of the chemicals used in this study were in analytical grade. Double-distilled water was used for the preparation of all solutions. [BMIm][PF6] was supplied by Himedia Laboratories Pvt. Ltd., India.

Apparatus

All electrochemical experiments were performed using MPG2 Biologic system (Biologic Sci. Ins., India) controlled by ECLab® software. A three-electrode cell was assembled with the fabricated electrode as the working electrode, a platinum plate as the counter electrode, and an Ag/AgCl reference electrode. All experiments were conducted at room temperature (27 °C). A 7800 ICP-MS system was operated according to the EPA 200.8 method.

Preparation of paste electrodes

Raw MWCNTs were heated at 350 °C for 6 h in nitrogen effluent to remove moisture and then used for electrode fabrication.

i) Preparation of [BMIm][PF6]/MWCNT electrodes. 0.5 g of MWCNTs was dispersed into *n*-hexane solvent in a covered beaker under ultrasonication for 5 min. Different amounts of [BMIm][PF6] were then added to this suspension, and the beaker was opened. The weight ratios of the [BMIm][PF6]:MWCNT were studied at 15:85, 20:80, 25:75 and 30:70. The mixture was continuously ultrasonicated until a paste form was formed. The fresh paste composite was carefully packed onto a 10 mm-deep perforated polytetrafluoroethylene rod with a 3 mm inner diameter. A copper wire was inserted into the capillary tube and served as the electrical contact component.

ii) Preparation of silicon/[BMIm][PF6]/MWCNT electrodes. The same procedure was performed, but silicon oil was added to the mixture along with [BMIm][PF6]. The desired weight ratios of silicon:[BMIm][PF6]:MWCNT were 20:0:80, 19:1:80, 15:5:80, 17:3:80 and 10:10:80. The obtained electrodes were labelled S-20/B-0, S-19/B-1, S-17/B-3, S-15/B-5 and S-10/B-10, respectively.

The electrode surface was renewed for each electrochemical performance by polishing on abrasive paper.

Electrochemical measurements

i) Cycle voltammetry (CV) measurements were performed in a 50 ml solution containing 0.1 M KCl and 50 mM $K_3Fe(CN)_6$. Linear weep voltammograms were recorded in a potential range from –0.2 to 1.0 V, with scan rates ranging from 10 to 200 mV s^{-1}. A nitrogen flow was

bubbled into the analytical solution to remove dissolved oxygen before starting a potential sweep.

ii) Electrochemical impedance spectroscopy (EIS) was recorded in the frequency range of 0.01−10 kHz using a single sinusoidal excitation with an amplitude of 10 mV. EIS measurements were performed in the electrolyte containing 0.1 M KCl and 50 mM $K_3Fe(CN)_6$.

iii) The linear sweep anodic stripping voltammetry (LSASV) method was applied to detect Pb^{2+} and Cd^{2+} in solutions with the following steps: Firstly, the metal ion was accumulated on the working electrode surface for deposition time at a deposition potential while the solution was stirred at 150 rpm. Next, the stirrer was stopped until the solution reached a resting state. After that, the potential was linearly swept from deposition potential to 0 V with a scan rate of 50 mV s^{-1}. The current was recorded during the scan, releasing an anodic stripping voltammogram. The LSASV measurements were performed for individual solutions of Pb^{2+} (1, 1.5, 4.5, 9, 18, 27 and 36 μg L^{-1}) and Cd^{2+} (0.5, 1.5, 3.5, 7, 10, 15 and 20 μg L^{-1}). The deposition time and the deposition potential for the LSASV performances were optimized in this study.

Determinations of Pb^{2+} and Cd^{2+} in real sample

Tap water was collected for determining Pb^{2+} and Cd^{2+} concentrations using the LSASV and ICP-MS methods. According to the standard addition method, 10 mL of Cd^{2+} solution (1.0 mg/L), 10 mL of Pb^{2+} solution (1.0 mg/L) and 7.45 g of KCl were transferred to a 1000 ml-volumetric flask and then adjusted to 1000 mL using a tap water sample. This solution was next adjusted to pH 4 using HNO_3 0.1 M solution. The obtained analytical solution was extracted three repeated times of Pb^{2+} and Cd^{2+} determinations.

RESULTS AND DISCUSSION

Electrochemical behavior of [BMIm][PF6]/MWCNT electrodes

Fig. 1 shows the CVs of the [BMIm][PF6]/MWCNT electrodes in 50 mM of $Fe(CN)_6]^{3-/4-}$ solution. The background responses of the electrodes were large due to the contribution of capacitive current generated by both the [BMIm][PF6] and MWCNTs at the electrode surface.[23,28] This behaviour is inconvenient in analytical applications because the large capacitive currents can obscure the electroanalytical signals (faradaic currents), especially at low analytic concentrations.[29–31] The redox peaks appeared most obviously at the electrode containing 20 % weight of [BMIm][PF6], with peak-to-peak separation (ΔE_p) of 455 mV. This is larger than the theoretical value of 59 mV, indicating that a multi-electron transfer process occurs at the [BMIm][PF6]/MWCNT electrode surface.[32,33] This is likely due to the trapping of ions and/or charges in the [BMIm][PF6] layer rather than their transfer to the solution.[34,35] This experimental result demonstrates that using [BMIm][PF6] alone as a conductive binder is insufficient to enhance the electrochemical signal. Further improvements are necessary to reduce the background capacitive current.

Electrochemical behavior of silicon/[BMIm][PF6]/MWCNT electrodes

As discussed above, the [BMIm][PF6]/MWCNT electrode turned out not to be satisfactory for electroanalytical applications. To mitigate the background

current, silicon oil was used along with [BMIm][PF6] as a pasting binder to fabricate electrodes. CV analyses were conducted to assess the enhancement of the electrochemical characteristics of the silicon/[BMIm][PF6]/MWCNT electrode.

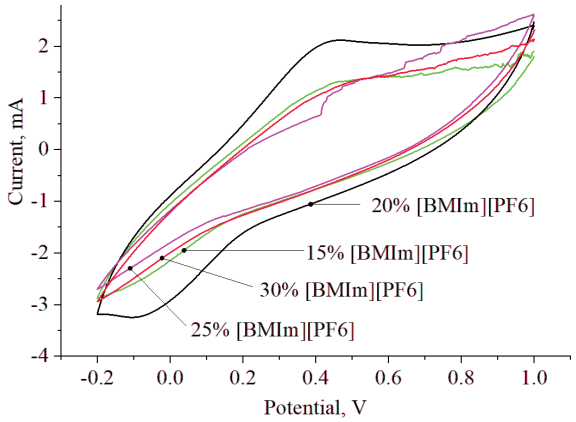

Fig. 1. Cyclic voltammograms of the [BM Im][PF6]/MWCNT electrodes (solution containing 0.1 M KCl and 50 mM $K_3[Fe(CN_6)]$, pH 4, scan rate: 20 mV s^{-1}).

It is known that [BMIm][PF6] molecules can cover and interact with the outside surface of MWCNTs *via* π-π interactions,[36] causing a thick interface layer between the electrode surface and electrolyte. As a result, the cyclic voltammograms obtained in the absence and presence of $Fe(CN)_6]^{3-/4-}$ (Fig. 2a and b, respectively) show that the non-faradaic current increased with the amounts of [BMIm][PF6] applied. As depicted in Fig. 2a, the S-20/B-0 electrode exhibits a significantly low background response, contrasting with the S10/B-10 electrode. However, the high charge conductivity nature of [BMIm][PF6] contributed to the enhancement of the signal response rate of the silicon/[BMIm][PF6]/MWCNT electrodes. As a result, the peak currents of the $Fe(CN)_6]^{3-/4-}$ redox couple were improved, as shown in Fig. 2b and Table I. The oxidation peaks occurred at 0.28 V and were unchanged at different electrodes. However, the reduction peaks were slightly shifted to the left with the increasing [BMIm][PF6] content, resulting in a larger ΔE_p. This trend is consistent with the previous reports for [C_4mpyrr][NTf_2]/bamboo-like MWCNT[31] and [BMIm][PF6]/graphite.[37]

The results in Table I show that increasing the amount of [BMIm][PF6] in the paste composite increases the i_{pa} and i_{pc} values, indicating a positive effect of [BMIm][PF6] on the electrochemical performance of the electrodes. The i_{pa}/i_{pc} ratios at the S-20/B-0, S-19/B-1, S-17/B-3, and S-15/B-5 electrodes are close to unity (1.034, 0.979, 1.022 and 0.945, respectively), while this ratio at the S-10/B--10 electrode is 0.826. The ΔE_p values for all five electrodes are in the range of 114–162 mV. These results suggest that the electron transfer processes at the

S-10/B-10 electrode are irreversible, while the processes at the other electrodes are quasi-reversible.[32,38] This finding indicates that the use of a mixture of silicon oil and [BMIm][PF6] as a paste binder can enhance the electrochemical properties of the electrode, compared to the use of silicon oil or [BMIm][PF6] alone.

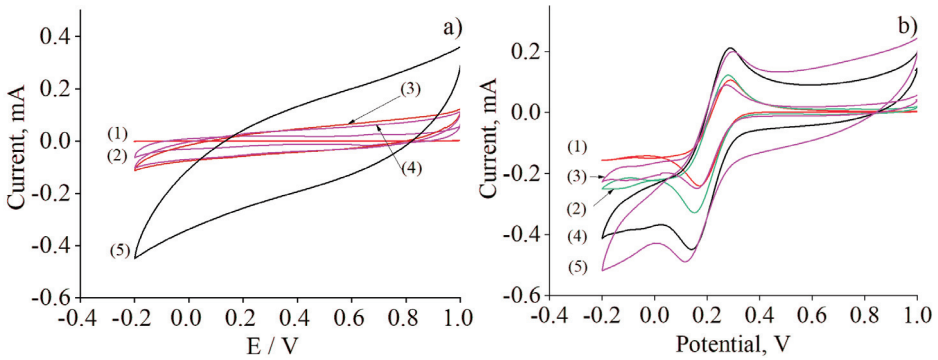

Fig. 2. CVs in solution of: a) 0.1 M KCl and b) 0.1 M KCl and 50 mM $K_3Fe(CN)_6$ at (1): S-20/B-0, (2): S-19/B-1, (3): S-17/B-3, (4): S-15/B-5 and (5) S-10/B-10 electrodes (pH 4, scan rate: 10 mV s^{-1}).

TABLE I. Results from CV measurements in solution of 0.1 M KCl and 50 mM $K_3Fe(CN)_6$ at silicon/[BMIm][PF6]/MWCNT electrodes (pH 4, scan rate of 10 mV s^{-1}); i_{pa} and i_{pc} are the oxidation and reduction peak currents

Parameter	Electrode				
	S-20/B-0	S-19/B-1	S-17/B-3	S-15/B-5	S-10/B-10
i_{pa} / μA	245	320	368	324	251
i_{pc} / μA	237	327	360	343	304
i_{pa}/i_{pc} ratio	1.034	0.979	1.022	0.945	0.826
ΔE_p / mV	114	130	152	155	162

The current response of the $Fe(CN_6)^{3-/4-}$ redox couple at the S-17/B-3 electrode was obviously higher than that of the other electrodes. As a result, the S-17/B-3 electrode was selected for the following electrochemical studies.

The S-17/B-3 electrode

i) Study on cyclic voltammetry. The electrochemical properties of the S-17/B-3 electrode were investigated using CV in $Fe(CN_6)^{3-/4-}$ solution at different potential sweep rates (v:10, 20, 30, 40, 50, 70, 100, 150 and 200 mV s^{-1}). The inset in Fig. 3a shows the recorded CVs, which reveals that the ΔE_p increases with v. This suggests that equilibrium at the electrolyte-electrode interface has not been reached.[39]

Fig. 3a shows linear relationships with a non-zero intercept between peak currents ($|i_p|$) and $v^{0.5}$, which is consistent with previous studies.[23,40] This

behaviour indicates that the electrochemical process at the S-17/B-3 electrode was a diffusion-controlled mechanism.[23,38] Additionally, the non-zero intercept of $|i_p| \sim v^{0.5}$ lines demonstrated the existence of spherical diffusion[41] and/or non-faradaic components[42] in the electrode processes. This is attributed to the nature of a non-planar electrode surface or the capacitive characteristics of the interfacial layer.[42–44] Furthermore, the $i_{pa} \sim v^{0.5}$ line was slightly steeper than the $-i_{pc} \sim v^{0.5}$ line, indicating that the quasi-reversible redox reactions of $Fe(CN_6)^{3-/4-}$ occurred at the electrode surface with a faster charge transfer rate in the oxidation process, compared to the reduction process.[45]

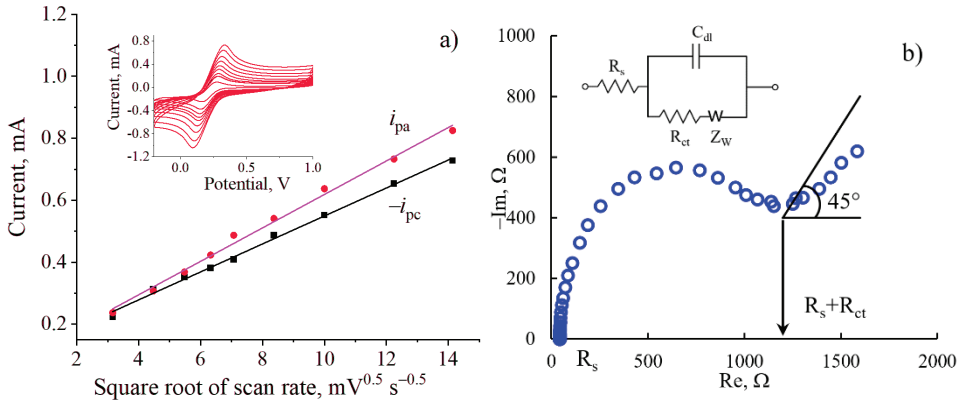

Fig. 3. a) Plots of peak currents against squared root of scan rate (the inset: cyclic voltammograms) and b) Nyquist plot (inset: equivalent circuit model). Electrolyte: 0.1 M KCl, 50 mM $K_3Fe(CN)_6$, pH 4.

ii) Study on electrochemical impedance spectroscopy. The characteristics of the electrode/electrolyte interface, including electron transfer resistance (R_{ct}), double layer capacitance (C_{dl}) and molecules/species diffusion (Z_W) were explored by EIS analysis.[46] As illustrated in Fig. 3b for the Nyquist plot, the EIS represents a semicircle in the mid-frequency range and a tail in the low-frequency range. The intercept between the semicircle and the real axis corresponds to the solution's electric resistance (R_s).[46] The Randles circuit (the inset in Fig. 3b) was preferred to fit the experimental impendence data, revealing R_s = 43.3 Ω, C_{dl} = = 0.46 mF, R_{ct} = 1004 Ω. A similar result was reported in the previous report.[47] The slope of the tail in the Nyquist plot is gentler than 45°, indicating the diffusion processes at a non-planar electrode surface.[48]

iii) Optimization of the LSASV conditions. The influence of solution pH on the Pb^{2+} and Cd^{2+} determinations was investigated. At low pH, the competition between H^+ and metal ions for the active sites at the electrode surface was more intense. Oppositely, it shifts to the hydrolysis of Pb^{2+} and Cd^{2+} at high pH, which results in the peak currents of Pb^{2+} and Cd^{2+} first increasing and then dec-

reasing with pH rising from 2 to 6, as presented in Fig. 4a. The highest peak current is achieved at pH 3 for Pb^{2+} and pH 5 for Cd^{2+}. Additionally, the stripping current of Pb^{2+} and Cd^{2+} at pH 4 deviated by 3.1 and 1.8 %, compared to the highest current, respectively. Therefore, pH 4 was considered for the following analysis.

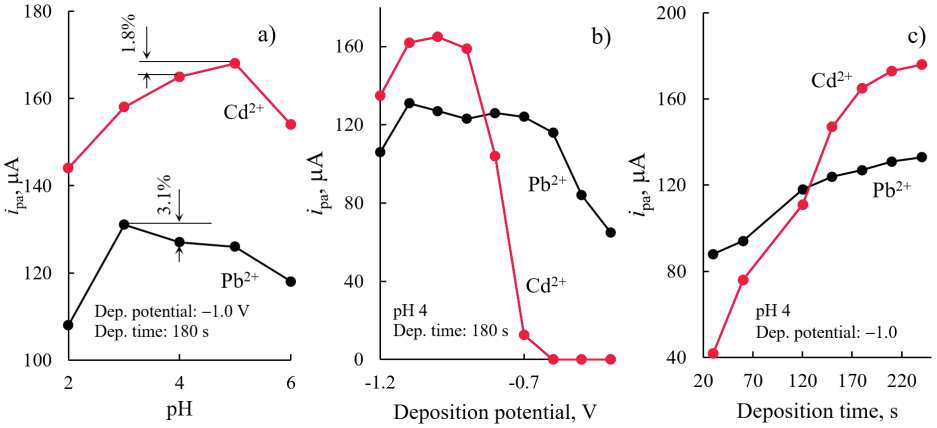

Fig. 4. Dependence of stripping peak current on: a) solution pH, b) deposition potential, c) deposition time (electrolyte: 0.1 M KCl, Pb^{2+}, 10 μg L^{-1}, Cd^{2+}, 10 μg L^{-1})

The dependence of the Pb^{2+} and Cd^{2+} stripping peak currents on the deposition potential ranging from −0.4 to −1.2 V was found and shown in Fig. 4b. The negative shift of the deposition potential from −0.4 to −1.0 V can improve the reduction of Pb^{2+} and Cd^{2+} on the electrode surface, resulting in an increase in the stripping peak current. However, water in acidic conditions can be electrolyzed at a potential less than −1.0 V, forming hydrogen atoms, which are firmly active intermediates. This led to the formation of metal hydrides, which then released cathode surface.[49] As a result, the deposited metal layer was corroded, interfering with signal response. Therefore, −1.0 V exhibits a suitable deposition potential for subsequent experiments.

As shown in Fig. 4c, the stripping peak currents of Pb^{2+} and Cd^{2+} noticeably increased with the deposition time up to 180 s. When the deposition time was prolonged, the deposition processes on the electrode surface tended to the equilibrium. Therefore, with 240 s of deposition time, the stripping peak currents of both Pb^{2+} and Cd^{2+} were only 1.07-fold higher compared with 180 s of deposition time. For balancing the signal intensity and the analysis time, 180 s was considered the deposition time for the electrochemical analysis of Pb^{2+} and Cd^{2+}.

As discussed above, the appropriate parameters of LSASV performance using the S-17/B-3 electrode for Pb^{2+} and Cd^{2+} determinations were found, parti-

cularly pH 4, deposition potential at −1.0 V and deposition time for 180 s. These conditions were applied for all following ASV experiments.

iv) Application for individual Pb^{2+} and Cd^{2+} determinations. In this study, the LSASV method was applied to determine the Pb^{2+} and Cd^{2+} concentrations in the ranges of 1–36 μg L^{-1} and 0.5–20 μg L^{-1}, respectively. Fig. 5 shows the LSASV voltammograms for different ion concentrations at a scan rate of 50 mV s^{-1}. The higher metal ion concentration resulted in a broader peak and a higher peak current. The stripping peak positions for Pb^{2+} and Cd^{2+} were well-defined at −0.36 and −0.64 V, respectively, and were unchanged with increasing ion concentration. These peaks appeared at more positive potentials than in previous studies.[21,50] This may be because Cd^{2+} and Pb^{2+} were chelated with $BMIIM^{+}$, resulting in a change in their redox status.[51–53]

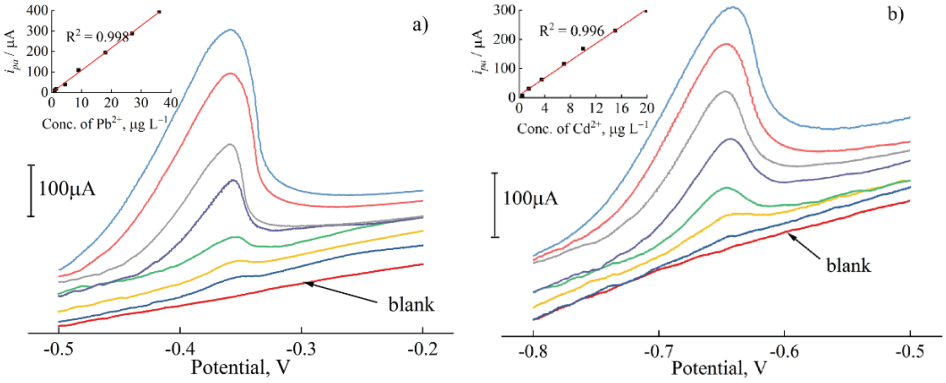

Fig. 5. The LSASV voltammograms for different concentrations of: a) Pb^{2+} and b) Cd^{2+} (scan rate: 50 mV s^{-1}, pH 4, deposition potential: −1.0 V, deposition time: 180 s). Insets: respective calibration plots for Pb^{2+} and Cd^{2+}.

For evaluating the applicability of the S-17/B-3 electrode for metal ions determination, linear regressions were performed between peak currents and ion concentrations. The insets in Fig. 5a and b show the calibration curves for Pb^{2+} and Cd^{2+}, respectively, which correspond to the following linear equations with R2 of 0.998 and 0.996, respectively.

The S-17/B-3 electrode exhibited a higher sensitivity to Cd^{2+} (14.7 μA $μg^{-1}$ L) than Pb^{2+} (10.9 μA $μg^{-1}$ L). The *LOD*s were found to be 2.25 μg L^{-1} for Pb^{2+} and 1.59 μg L^{-1} for Cd^{2+}, according to the 3σ criterion (n = 7). These *LOD*s are lower than the acceptable limits for Pb^{2+} (10 μg L^{-1}) and Cd^{2+} (3 μg L^{-1}) in drinking water, according to the WHO guidelines. Therefore, the proposed electrode suits Pb^{2+} and Cd^{2+} determinations in real applications.

The accuracy of the electrode was verified by comparing the analytical results from LSASV with those from ICP-MS for individual solutions of Pb^{2+} or

Cd^{2+}. Three simulated solutions of Pb^{2+} (10 μg L^{-1}) and Cd^{2+} (10 μg L^{-1}) in 0.1 M KCl solution (pH 4) were tested, illustrating results in Table II.

TABLE II. Concentrations of Pb^{2+} and Cd^{2+} in simulated solutions by the LSASV and ICP-MS methods

Method	Simulated sample			Mean	*RSD* / %
	#1	#2	#3		
	For Pb^{2+} determination				
LSASV	10.12	9.74	9.53	10.17	5.68
ICP-MS	9.86	9.93	9.90	9.90	0.35
	For Cd^{2+} determination				
LSASV	9.64	9.84	9.58	9.69	1.41
ICP-MS	9.78	9.82	9.86	9.82	0.41

The mean concentrations of Pb^{2+} and Cd^{2+} in simulated solutions were determined to be 10.17 and 9.69 μg L^{-1} with the LSASV method, and 9.90 and 9.82 μg L^{-1} with the ICP-MS method, respectively. In small values of the relative standard deviations (*RSD*s), the ICP-MS method exhibits a high-reliability method for Pb^{2+} and Cd^{2+} determinations and was used as the standard method in this study. The difference between the results from LSASV and ICP-MS was –4.3 % for Pb^{2+} and –6.0 % for Cd^{2+}, indicating the considerable applicability of S-17/B-3 electrode for monitoring Pb^{2+} and Cd^{2+}.

v) Repeatability, reproducibility and stability. Six individual solutions of Pb^{2+} and Cd^{2+} (10 μg L^{-1}) in 0.1 M KCl (pH 4) were prepared for the repetitive measurements using the LSASV method with the S-17/B-3 working electrode. The peak currents for Pb^{2+} (108, 104, 98, 106, 110 and 105 μA) and Cd^{2+} (157, 146, 161, 155, 148 and 152 μA) were recorded, revealing RSDs of 3.9 % for Pb^{2+} and 3.7 % for Cd^{2+}. Four different S-17/B-3 electrodes were fabricated following the identified procedure to assess the reproducibility. These electrodes were applied to determine the concentrations of Pb^{2+} and Cd^{2+} solutions at 10 μg L^{-1}. The *RSD*s were found to be 4.8 % for Pb^{2+} and 2.5% for Cd^{2+}. The S-17/B-3 electrode was also stored at room temperature (25–35 °C), at 60–80 % relative humidity, and without exposure to sunlight. Compared to the new electrode, the stripping peak currents at the electrode stored for 25 and 28 days declined by 3.4 and 7.6 % for Pb^{2+} and 2.1 and 3.2 % for Cd^{2+}, respectively. These results indicate that the S-17/B-3 electrode can be used to determine trace concentrations of Pb^{2+} and Cd^{2+} in aqueous solutions.

vi) Interference study. Common ions in tap water, such as Na^+, NH_4^+, Cu^{2+}, Ca^{2+}, Cl^-, F^-, NO_3^-, HCO_3^-, were added into the electrolyte containing 10 μg L^{-1} of Cd^{2+} or Pb^{2+} for the interference investigations. With ±5 % tolerable error, the maximum concentrations of the interfering salts were determined, as shown in Table III. The presence of Cl^-, F^- is not suitable for Pb^{2+} determination

due to the formation of weak dissociative $PbCl_2$ and PbF_2 forms. The Cd^{2+} determination has been interfered with in a wide range of interfering concentrations.

TABLE III. Effect of interferences on the individual determinations of Pb^{2+} (10 μg L^{-1}) and Cd^{2+} (10 μg L^{-1})

Interference (concentration range)	Highest concentration of interference with ±5 % tolerable error	
	For Pb^{2+} determination	For Cd^{2+} determination
NaCl (25–2000 mg/L)	Not suitable	500
$NaNO_3$ (25–2000 mg/L)	1000	1000
NaF (1–20 mg/L)	Not suitable	1
$NaHCO_3$ (50–500 μg/L)	200	100
NH_4Cl (100–500 μg/L)	Not suitable	500
$Pb(NO_3)_2$ (100–500 μg/L)	Non test	200
$Cd(NO_3)_2$ (100–500 μg/L)	300	Non test
$Cu(NO_3)_2$ (50–500 μg/L)	500	500
$Ca(NO_3)_2$ (5–500 mg/L)	500	500

vii) Application for real sample. The collected sample was used to prepare electrolytes containing 0.1 M KCl, 10 μg L^{-1} of Pb^{2+} and 10 μg L^{-1} of Cd^{2+} (pH 4) for LSASV and ICP-MS analyses. As presented in Table IV, the difference of the found Pb^{2+} and Cd^{2+} concentrations by LSASV and ICP-MS was less than 5 %. This result indicates that the S-17/B-3 electrode can provide good accuracy and reliability for the Pb^{2+} and Cd^{2+} determinations using the LSASV method.

TABLE IV. Concentrations of Pb^{2+} and Cd^{2+} in working solutions prepared from tap water medium

Method	Added, μg L^{-1}	Found, μg L^{-1}			Mean
		#1	#2	#3	
		For Pb^{2+}			
LSASV	10	13.05	12.86	12.92	12.94
ICP-MS	10	12.42	13.55	13.21	13.06
		For Cd^{2+}			
LSASV	10	10.12	10.37	10.03	10.17
ICP-MS	10	10.42	10.55	10.61	10.53

CONCLUSION

The MWCNT PEs were fabricated in the presence of [BMIm][PF6]. The [BMIm][PF6]/MWCNT PE exhibited high non-faradaic components, making it unacceptable for analytical applications. However, the electrochemical behaviour of the electrode was improved using the pasting mixture of silicon oil and [BMIm][PF6]. Increasing the amount of [BMIm][PF6] increased both the charge transfer rate and background response. At a mass ratio of silicon oil to [BMIm][PF6] of 17:3, the corresponding S-17/B-3 electrode was the most suitable for determining Pb^{2+} and Cd^{2+} concentrations, using LSASV method. The

influence of solution pH, deposition potential, and deposition time were studied. Under optimal conditions, the linear relationships between the analytical responses and concentrations of Pb^{2+} (1–36 μg L^{-1}) or Cd^{2+} (0.5–20 μg L^{-1}) were expressed. The low detection limits, good accuracy, high repeatability, reproducibility, and stability of the proposed electrode demonstrated its applicability to determining Pb^{2+} and Cd^{2+} traces in solutions. However, the results from interference studies showed that the signal response for Pb^{2+} was significantly interfered with by Cl^- and F^-. The concentrations of Pb^{2+} and Cd^{2+} in tap water were successfully determined at the S-17/B-3 electrode with high consistency to results from ICP-MS method.

Acknowledgement. We acknowledge Ho Chi Minh City University of Technology (HCMUT), VNU-HCM for supporting this study.

ИЗВОД

ЕЛЕКТРОДА ОД УГЉЕНИЧНЕ ПАСТЕ ТИПА [BMIM][PF6]/СИЛИКОНСКО УЉЕ/ВИШЕСЛОЈНЕ УГЉЕНИЧНЕ НАНОЦЕВИ: ЕЛЕКТРОХЕМИЈСКА СВОЈСТВА И ПРИМЕНА ЗА ОДРЕЂИВАЊЕ ЈОНА ОЛОВА И КАДМИЈУМА

HAI D. TRAN[1], UYEN P. N. TRAN[2] и DINH QUAN NGUYEN[3,4]

[1]Faculty of Environment, Ho Chi Minh University of Natural Resources and Environment, Ho Chi Minh city, Vietnam, [2]Faculty of Engineering and Technology, Van Hien University, Ho Chi Minh City, Vietnam, [3]Laboratory of Biofuel and Biomass Research, Faculty of Chemical Engineering, Ho Chi Minh City University of Technology (HCMUT), 268 Ly Thuong Kiet, District 10, Ho Chi Minh City, Vietnam и [4]Vietnam National University Ho Chi Minh City, Linh Trung Ward, Thu Duc District, Ho Chi Minh City, Vietnam

Електроаналитичке методе су развијене за широку област примена, а посебно за детекцију трагова метала. У овом раду је испитана могућност примене јонске течности 1-бутил-3-метилимидазолијум хексафлурофосфата ([BMIm][PF6]) као везива у електроди од пасте вишеслојних угљеничних наноцеви за детекцију Pb^{2+} и Cd^{2+}. Електрохемијска својства електрода су испитана методама цикличне волтаметрије, спектроскопије електрохемијске импеданције и анодне линеарне волтаметрије. Коришћењем самог [BMIm][PF6] као везива није добијена електрода задовољавајућих карактеристика за електрохемијску анализу. Међутим, паста од угљеничних наноцеви за силиконским уљем и [BMIm][PF6] је показала одличну осетљивост за одређивање Pb^{2+} и Cd^{2+}, са границама детекције од 2,25 и 1,59 μg L^{-1}, редом. Предложена електрода се показала као поуздан сензор за тачно квантитативно одређивање јона Pb^{2+} и Cd^{2+} у траговима, испољавајући добру поновљивост, репродуктивност и стабилност.

(Примљено 22. јуна, ревидирано 21. јула, прихваћено 11. децембра 2023)

REFERENCES

1. M. Jaishankar, T. Tseten, N. Anbalagan, B. B. Mathew, *Interdiscip. Toxicol.* **7** (2014) 60-72 (https://doi.org/10.2478/intox-2014-0009)
2. M. Balali-Mood, K. Naseri, Z. Tahergorabi, M. R. Khazdair, M. Sadeghi, *Front. Pharmacol.* **12** (2021) 227 (https://doi.org/10.3389/fphar.2021.643972)
3. X. Yang, J. Yan, F. Wang, J. Xu, X. Liu, K. Ma, X. Hu, J. Ye, *J. Serb. Chem. Soc.* **81** (2016) 697 (https://doi.org/10.2298/10.2298/JSC151124011Y)

4. M. E. Morales, R. S. Derbes, C. M. Ade, J. C. Ortego, J. Stark, P. L. Deininger, A. M. Roy-Engel, *PloS One* **11** (2016) e0151367 (https://doi.org/10.1371/journal.pone.0151367)
5. B. K. Bansod, T. Kumar, R. Thakur, S. Rana, I. Singh, *Biosens. Bioelectron.* **94** (2017) 443 (https://doi.org/10.1016/j.bios.2017.03.031)
6. E. C. Okpara, O. E. Fayemi, O. B. Wojuola, D. C. Onwudiwe, E. E. Ebenso, *RSC Adv.* **12** (40) (2022) 26319 (https://doi.org/10.1039/D2RA02733J)
7. J. Lv, Y. Tang, L. Teng, D. Tang, J. Zhang, *J. Serb. Chem. Soc.* **82** (2017) 73 (https://doi.org/10.2298/JSC160419090L)
8. O. A. Farghaly, R. A. Hameed, A.-A. H. Abu-Nawwas, *Int. J. Electrochem. Sci.* **9** (2014) 3287 (http://www.electrochemsci.org/papers/vol9/90603287.pdf).
9. J. M. Díaz-Cruz, N. Serrano, C. Pérez-Ràfols, C. Ariño, M. Esteban, *J. Solid State Electrochem.* **24** (2020) 2653 (http://doi.org/10.1007/s10008-020-04733-9)
10. C. Apetrei, I. M. Apetrei, J. A. D. Saja, M. L. Rodriguez-Mendez, *Sensors* **11** (2) (2011) 1328 (https://doi.org/10.3390/s110201328)
11. R. Rejithamol, S. Beena, *Front. Sens.* **3** (2022) 901628 (https://doi.org/10.3389/fsens.2022.901628)
12. A. J. Slate, D. A. Brownson, A. S. A. Dena, G. C. Smith, K. A. Whitehead, C. E. Banks, *Phys. Chem. Chem. Phys.* **20** (2018) 20010 (https://doi.org/10.1039/C8CP02196A)
13. J. Wang, Ü. A. Kirgöz, J.-W. Mo, J. Lu, A. N. Kawde, A. Muck, *Electrochem. Commun.* **3** (2001) 203 (https://doi.org/10.1016/S1388-2481(01)00142-4)
14. R.-l. Stefan, S. G. Bairu, *Talanta* **63** (2004) 605 (https://doi.org/10.1016/j.talanta.2003.12.023)
15. S. Motoc, F. Manea, C. Orha, A. Pop, *Sensors* **19** (6) (2019) 1332 (https://doi.org/10.3390/s19061332)
16. M. D. Rubianes, G. A. Rivas, *Electrochem. Commun.* **5** (2003) 689 (https://doi.org/10.1016/S1388-2481(03)00168-1)
17. K. Gong, Y. Yan, M. Zhang, L. Su, S. Xiong, L. Mao, *Anal. Sci.* **21** (2005) 1383 (http://doi.org/10.2116/analsci.21.1383)
18. C. L. Brito, E. I. Ferreira, M. A. La-Scalea, *Electrochi. Acta* **459** (2023) 142486 (https://doi.org/10.1016/j.electacta.2023.142486)
19. K. Fan, J. Wu, *Anal. Methods* **5** (2013) 5146 (https://doi.org/10.1039/C3AY40997J)
20. X. Guo, Y. Yun, V. N. Shanov, H. B. Halsall, W. R. Heineman, *Electroanalysis* **23** (2011) 1252 (https://doi.org/10.1002/elan.201000674)
21. C. R. T. Tarley, V. S. Santos, B. E. L. Baêta, A. C. Pereira, L. T. Kubota, *J Hazard. Mater.* **169** (2009) 256 (https://doi.org/10.1016/j.jhazmat.2009.03.077).
22. T.L. Hai, T.D. Hai, in *Proceedings of the 3rd International Conference on Chemical Engineering, Food and Biotechnology*, AIP Conference Proceedings **1878** (2017) 020023 (https://doi.org/10.1063/1.5000191)
23. H. Liu, P. He, Z. Li, C. Sun, L. Shi, Y. Liu, G. Zhu, J. Li, *Electrochem. Commun.* **7** (2005) 1357 (https://doi.org/10.1016/j.elecom.2005.09.018).
24. J. Ping, J. Wu, Y. Ying, M. Wang, G. Liu, M. Zhang, *J. Agric. Food Chem.* **59** (2011) 4418 (https://doi.org/10.1021/jf200288e).
25. H. Bagheri, A. Afkhami, H. Khoshsafar, M. Rezaei, A. Shirzadmehr, *Sens. Actuators, B* **186** (2013) 451 (https://doi.org/10.1016/j.snb.2013.06.051)

26. M. Yang, T.-J. Jiang, Z. Guo, J.-H. Liu, Y.-F. Sun, X. Chen, X.-J. Huang, *Sens. Actuators, B* **240** (2017) 887 (https://doi.org/10.1016/j.snb.2016.09.060).
27. L. Oularbi, M. Turmine, F. E. Salih, M. E. Rhazi, *J. Environ. Chem. Eng.* **8** (2020) 103774 (https://doi.org/10.1016/j.jece.2020.103774)
28. J. N. Barisci, G. G. Wallace, R. H. Baughman, *J. Electroanal. Chem.* **488** (2000) 92 (https://doi.org/10.1016/S0022-0728(00)00179-0).
29. C. Sandford, M. A. Edwards, K. J. Klunder, D. P. Hickey, M. Li, K. Barman, M. S. Sigman, H. S. White, S. D. Minteer, *Chem. Sci.* **10** (2019) 6404 (https://doi.org/10.1039/C9SC01545K)
30. S. G. Hernández-Vargas, C. A. Cevallos-Morillo, J. C. Aguilar-Cordero, *Electroanalysis* **32** (2020) 1938 (https://doi.org/10.1002/elan.201900701)
31. R. T. Kachoosangi, G. G. Wildgoose, R. G. Compton, *Electroanalysis* **19** (2007) 1483 (https://doi.org/10.1002/elan.200703883).
32. N. Elgrishi, K. J. Rountree, B. D. McCarthy, E. S. Rountree, T. T. Eisenhart, J. L. Dempsey, *J. Chem. Educ.* **95** (2018) 197 (https://doi.org/10.1021/acs.jchemed.7b00361)
33. M. Sýs, E. Khaled, R. Metelka, K. Vytřas, *J. Serb. Chem. Soc.* **82** (2017) 865 (https://doi.org/10.2298/JSC170207048S)
34. G. Shul, J. Sirieix-Plenet, L. Gaillon, M. Opallo, *Electrochem. Commun.* **8** (2006) 1111 (https://doi.org/10.1016/j.elecom.2006.05.002)
35. K. Kirchner, T. Kirchner, V. Ivaništšev, M. V. Fedorov, *Electrochim. Acta* **110** (2013) 762 (https://doi.org/10.1016/j.electacta.2013.05.049)
36. N. Maleki, A. Safavi, F. Tajabadi, *Anal. Chem.* **78** (2006) 3820 (https://doi.org/10.1021/ac060070+)
37. M. Musameh, J. Wang, *Anal. Chim. Acta* **606** (2008) 45 (https://doi.org/10.1016/j.aca.2007.11.012)
38. Y. Zhang, J. B. Zheng, *Electrochim. Acta* **52** (2007) 7210 (https://doi.org/10.1016/j.electacta.2007.05.039)
39. J.-Y. Lu, Y.-S. Yu, T.-B. Chen, C.-F. Chang, S. Tamulevičius, D. Erts, K. C.-W. Wu, Y. Gu, *Polymers* **13** (2021) 343 (https://doi.org/10.3390/polym13030343)
40. M. B. Gholivand, A. Azadbakht, *Electrochim. Acta* **56** (2011) 10044 (https://doi.org/10.1016/j.electacta.2011.08.098)
41. O. A. González-Meza, E. R. Larios-Durán, A. Gutiérrez-Becerra, N. Casillas, J. I. Escalante, M. Bárcena-Soto, *J. Solid State Electrochem.* **23** (2019) 3123 (http://doi.org/10.1007/s10008-019-04410-6)
42. P. Monk, in *Fundamentals of Electro-Analytical Chemistry*, P. Monk, Ed., John Wiley & Sons Ltd., Chichester, 2001, p 131 (https://doi.org/10.1002/9780470511329.ch6)
43. T. Tichter, J. Schneider, C. Roth, *Front. Energy Res.* **8** (2020) 155 (https://doi.org/10.3389/fenrg.2020.00155)
44. J. S. Čović, A. R. Zarubica, A. L. Bojić, T. M. Troter, M. S. Ranđelović, *J. Serb. Chem. Soc.* **85** (2020) 1185 (https://doi.org/10.2298/JSC200221043C)
45. C. O. Laoire, E. Plichta, M. Hendrickson, S. Mukerjee, K. M. Abraham, *Electrochim. Acta* **54** (26) (2009) 6560 (https://doi.org/10.1016/j.electacta.2009.06.041)
46. H. S. Magar, R. Y. Hassan, A. Mulchandani, *Sensors* **21** (19) (2021) 6578 (https://doi.org/10.3390/s21196578)
47. M. S. Ahmad, I. M. Isa, N. Hashim, S. M. Si, M. I. Saidin, *J. Solid State Electrochem.* **22** (2018) 2691 (http://doi.org/10.1007/s10008-018-3979-y)

48. A. C. Lazanas, M. I. Prodromidis, *ACS Meas. Sci. Au* **3** (3) (2023) 162 (https://doi.org/10.1021/acsmeasuresciau.2c00070)
49. T. Wirtanen, T. Prenzel, J.-P. Tessonnier, S. R. Waldvogel, *Chem. Rev.* **121** (2021) 10241 (https://doi.org/10.1021/acs.chemrev.1c00148)
50. D. Zhao, X. Guo, T. Wang, N. Alvarez, V. N. Shanov, W. R. Heineman, *Electroanalysis* **26** (2014) 488 (https://doi.org/10.1002/elan.201300511)
51. M. Tian, L. Fang, X. Yan, W. Xiao, K. H. Row, *J. Anal. Methods Chem.* **2019** (2019) 1948965 (https://doi.org/10.1155/2019/1948965)
52. C. M. Simonescu, V. Lavric, A. Musina, O. M. Antonescu, D. C. Culita, V. Marinescu, C. Tardei, O. Oprea, A. M. Pandele, *J. Mol. Liq.* **307** (2020) 112973 (https://doi.org/10.1016/j.molliq.2020.112973)
53. R. Nazar, N. Iqbal, A. Masood, M. I. R. Khan, S. Syeed, N. A. Khan, *Am. J. Plant Sci.* **3** (2012) 1476 (http://doi.org/10.4236/ajps.2012.310178).